

Influence of Scan Parameters of Single and Dual-Energy CT Protocols in Combination with Metal Artifact Suppression Algorithms for THA

An ex Vivo Study

Gilbert M. Schwarz, MD, Stephanie Huber, MD, Christian Wassipaul, MD, Maximilian Kasparek, MD, PhD, Lena Hirtler, MD, PhD, Jochen G. Hofstaetter, MD, Till Bader, MD, and Helmut Ringl, MD

Background: Metal artifacts caused by hip arthroplasty stems limit the diagnostic value of computed tomography (CT) in the evaluation of periprosthetic fractures or implant loosening. The aim of this ex vivo study was to evaluate the influence of different scan parameters and metal artifact algorithms on image quality in the presence of hip stems.

Methods: Nine femoral stems, 6 uncemented and 3 cemented, that had been implanted in subjects during their lifetimes were exarticulated and investigated after death and anatomical body donation. Twelve CT protocols consisting of single-energy (SE) and single-source consecutive dual-energy (DE) scans with and without an iterative metal artifact reduction algorithm (iMAR; Siemens Healthineers) and/or monoenergetic reconstructions were compared. Streak and blooming artifacts as well as subjective image quality were evaluated for each protocol.

Results: Metal artifact reduction with iMAR significantly reduced the streak artifacts in all investigated protocols ($p = 0.001$ to 0.01). The best subjective image quality was observed for the SE protocol with a tin filter and iMAR. The least streak artifacts were observed for monoenergetic reconstructions of 110, 160, and 190 keV with iMAR (standard deviation of the Hounsfield units: 151.1, 143.7, 144.4) as well as the SE protocol with a tin filter and iMAR (163.5). The smallest virtual growth was seen for the SE with a tin filter and without iMAR (4.40 mm) and the monoenergetic reconstruction of 190 keV without iMAR (4.67 mm).

Conclusions: This study strongly suggests that metal artifact reduction algorithms (e.g., iMAR) should be used in clinical practice for imaging of the bone-implant interface of prostheses with either an uncemented or cemented femoral stem. Among the iMAR protocols, the SE protocol with 140 kV and a tin filter produced the best subjective image quality. Furthermore, this protocol and DE monoenergetic reconstructions of 160 and 190 keV with iMAR achieved the lowest levels of streak and blooming artifacts.

Level of Evidence: Diagnostic Level III. See Instructions for Authors for a complete description of levels of evidence.

Osteoarthritis is the most common joint disorder in the United States¹ and Europe². As a result, total hip arthroplasties (THAs) and hip hemiarthroplasties are among the most frequent orthopaedic procedures³. While radiographs remain the workhorses in postoperative imaging, computed tomography (CT) scans are the standard of care in cases of prosthetic loosening or periprosthetic fractures⁴. However, interpretation of the bone-implant interface on diagnostic imaging remains challenging, since metal-related artifacts limit the diagnostic accuracy of CT scans in these patients^{5,6}.

The most important metal-related artifacts are beam-hardening artifacts. These include streak artifacts, which are dark streaks around dense structures and between multiple such

structures⁷. In addition, blooming artifacts due to photon starvation and beam-hardening artifacts make prostheses appear larger than they are. Smoothing filter kernels may artificially increase the attenuation of the tissue surrounding high-density metal objects (e.g., femoral stems) and virtually exaggerate their size⁸. These artifacts impair the visibility of the bone-implant interface and the interpretation of CT scans⁷.

A number of strategies have been proposed to reduce metal artifacts, including various single-energy (SE) and dual-energy (DE) CT protocols as well as combined DE and iterative monoenergetic protocols⁸⁻¹⁴. The majority of the available iterative metal artifact reduction (MAR) algorithms use an image-based metal segmentation method⁶. Pixels suspected to contain

Disclosure: The **Disclosure of Potential Conflicts of Interest** forms are provided with the online version of the article (<http://links.lww.com/JBJS/H437>).

metal on uncorrected images are segmented on the basis of a Hounsfield unit (HU) threshold. Images are then forward-projected to identify the corrupted projection data, which are removed and interpolated with appropriate estimations based on uncorrupted projection data. Finally, the interpolated sinogram is reconstructed to generate a corrected image.

The severity of metal artifacts is dependent not only on the CT protocol but also on the material of the implant. Hip implants are primarily designed to guarantee stable secondary long-term fixation due to osseointegration rather than to minimize metal artifacts¹⁵. Current femoral stems in hip implants mainly consist of titanium or stainless-steel alloys and, due to the high survival of THA implants, these implants and the metal artifacts caused by them will be encountered by clinical radiologists and orthopaedic surgeons for a long time to come.

The aim of this *ex vivo* study was to evaluate the influence of different scan parameters and metal artifact algorithms on image quality in the presence of hip stems. Our hypothesis was that a protocol using MAR, a tin filter, and monoenergetic reconstruction would reduce metal artifacts around hip stems and positively influence image quality. We further hypothesized significant differences in streak and blooming artifacts between uncemented and cemented stem types.

Materials and Methods

All specimens originated from the Vienna Medical Bio-/Implantbank of the Center for Anatomy and Cell Biology of the Medical University of Vienna. Prior to their death, all donors had provided informed written consent to have their bodies used in medical education and research. Approval by the institutional review board of the Medical University of Vienna (EK 1723/2018) was obtained for their use in this *ex vivo* study. The study involved 9 femora with hip prostheses that had been implanted during the person's lifetime and therefore provided a realistic representation of implant osseointegration. Standard and short uncemented stems as well as standard cemented stems were included if there were no signs or history of fracture or revision (Fig. 1). Because lysis of the bone-implant interface, a potential sign of septic or aseptic loosening, may occur after any duration of implantation, the time that the selected specimens had been *in situ* ranged from 1.8 to 307.1 months, in order to represent a broad range of bone ingrowth stages. The mean age of the donors was 86 ± 7.2 years, which is comparable to the reported peak of periprosthetic fractures in the average population at a mean age of 88 years¹⁶. Each femur was exarticulated and was stored at -20°C . Three areas of interest were defined on the basis of the Gruen zones¹⁷ (Fig. 2): cross-sectional area 1 (Gruen zones 1 and 7), cross-sectional area 2 (Gruen zones 2 and 6), and cross-sectional area 3 (Gruen zones 3 and 5).

CT Scan Protocols

All scans were performed with a DE, multidetector CT scanner (Siemens Somatom Edge Plus; Siemens Healthineers) routinely used in the clinical setting for fracture detection and preoperative planning prior to revision surgery.

Based on previous studies and our preliminary results indicating that they had the best performance for the included

prostheses (Fig. 3), 12 CT protocols were compared. Each femur was placed in a standardized box ($60 \times 40 \times 32$ cm) filled with 40 L of water to simulate surrounding soft tissue^{8,14}. The water bath mimicked the surroundings of the prostheses with a thigh-equivalent diameter of water. Dose modulation (CARE Dose; Siemens Healthineers) was active for all protocols, and the reference mAs value was adapted for each protocol (range, 150 to 357.9) to keep the total radiation dose (mean dose length product [DLP]) approximately constant among the scan protocols, to avoid a dose-dependent bias regarding metal artifacts (Table I). The applied mAs values were similar to published literature¹⁸. Since the same amount of water was used for all patients CARE Dose adapted the individual radiation based on the femur size. All scans were reconstructed in the transverse orientation at the previously defined areas of interest (Gruen zones 1 and 7, 2 and 6, 3 and 5) using a slice thickness of 0.6 mm and a slice interval of 0.6 mm. DE scans were acquired using single-source CT with 2 consecutive scans at 80 and 140 kV, and mixed images of these 2 voltages were reconstructed SE scans used only 140 kV with and without a tin filter. The DE scans were performed with and without monoenergetic image reconstruction with 110, 160, and 190 keV (Monoenergetic Plus; Siemens Healthineers), based on previous studies that demonstrated promising results in terms of MAR for these keV levels^{12,13}. In addition, all SE and DE scans were reconstructed with and without an iterative MAR algorithm (iMAR; Siemens Healthineers).

Quantitative Image Analysis

All image analyses were performed with standard DICOM (digital imaging and communications in medicine) viewer software (RadiAnt DICOM Viewer, version 2021.2.2; Medixant) using a monitor calibrated according to the DICOM standard in an environment with subdued lightning. The viewing window width and level were kept constant at a bone window (width = 400, level = 1,800) throughout image analysis.

Two readers (orthopaedic surgeons), who were blinded to the protocol and each other's results, individually measured streak and blooming artifacts for each prosthesis and protocol. Both were trained prior to the study on how to perform these measurements on sample slices. To quantify the streak artifacts around the implant, 6 regions of interest (ROIs) were positioned around the prosthesis as previously described⁸, to represent a simplified circular line-density profile by means of a few averaged sample points (Fig. 2). As far as possible, all regions of a single slice were placed in the same tissue or phantom material (cortical bone, cancellous bone, or water), resulting in a low standard deviation (SD) among these 6 regions. Streak artifacts in close vicinity to the prosthesis will considerably reduce (dark streaks) or increase (bright streaks) the mean attenuation (measured in HUs) of at least 1 of these 6 regions and thus increase the SD for this set of regions. Each ROI consisted of several pixels to ensure that streak artifacts were the main factor influencing the SD. Consequently, in this manuscript, the SD is used as the quantitative measurement of streak artifacts.

To quantify the virtual growth of the stem (blooming artifact) for each protocol, the apparent stem size was measured

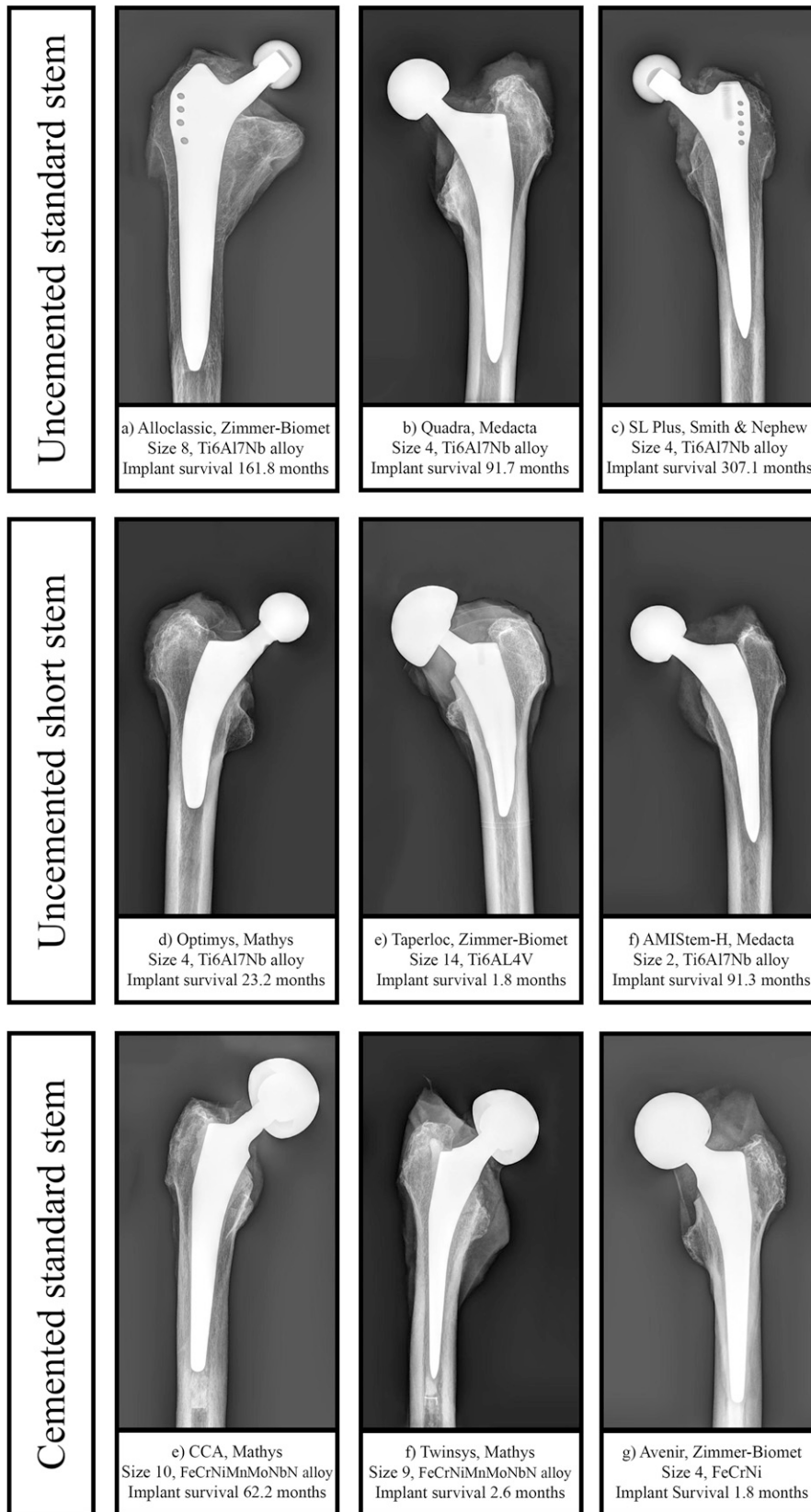


Fig. 1
Overview of the included prostheses.

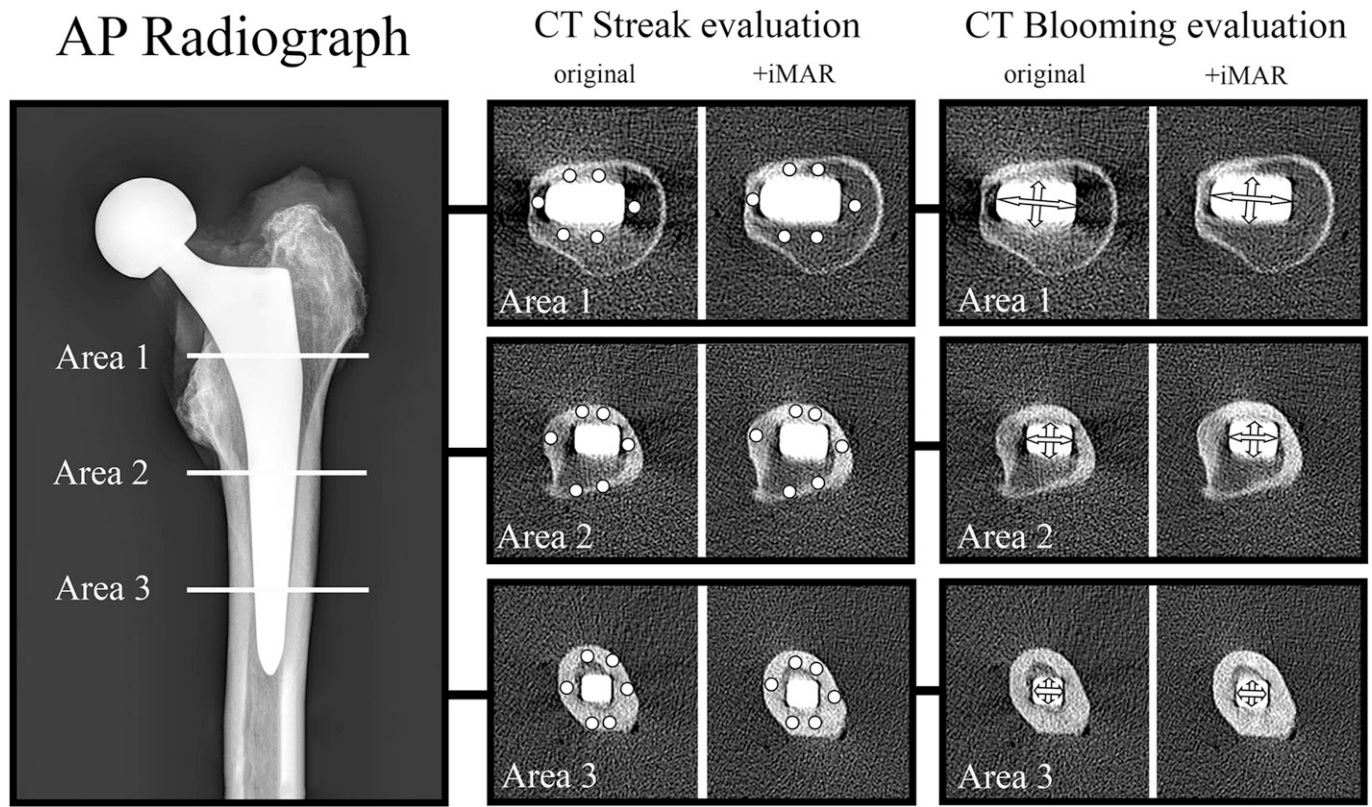


Fig. 2
Left: Anteroposterior (AP) radiograph of a representative specimen. Right: Sites or dimensions used for evaluating streak and blooming artifacts at each area of interest.

in anteroposterior and mediolateral directions. This apparent size was then compared with the results of our x-ray analysis and the manufacturer's specifications. The mean of the length measurements made by the readers was used for analysis.

Qualitative Image Analysis

Five readers (3 orthopaedic surgeons and 2 radiologists) independently graded all reconstructions for all prostheses for overall image quality and visibility of the periprosthetic boundary (i.e., the bone-implant interface) on a 5-point Likert scale (1: very good, 2: good, 3: intermediate, 4: poor, 5: very poor). The reconstructions were ranked from 1 (best) to 12 (worst) according to the readers' subjective evaluations of image quality. The readers were blinded to each others' evaluations as well as to the protocol and the type of prosthesis, as in previous studies⁸. In these qualitative image evaluations, the window level and width were freely adjustable by the individual reader.

Statistical Analysis

Statistical analyses were performed with IBM SPSS Statistics for Windows (version 25.0) and Microsoft Excel 365. Descriptive statistics (mean, SD, minimum, maximum) were computed for all continuous metric variables (blooming and streak artifacts). Differences between scan protocols were evaluated using a paired t test, and differences between stem types were assessed using 1-way analysis of variance (ANOVA). A p value of <0.05 was defined as

significant. When an ANOVA p value was significant, a post-hoc Tukey test was conducted to identify the pairs of means that differed significantly. The interrater reliability of the assessments of blooming and streak artifacts was calculated using the intraclass correlation coefficient (ICC)¹⁹. The interrater correlation was strong for blooming (ICC = 0.99) and streak artifacts (ICC = 0.96).

Source of Funding

There was no external source of funding for this study.

Results

Impact of Applied Protocol on Streak Artifacts

The lowest level of streak artifacts was observed for monoenergetic reconstructions of 160, 190, and 110 keV with iMAR (protocols 11, 12, 10) and the SE protocol with a tin filter and iMAR (protocol 4). Differences were significant compared with the mixed DE protocol (80 and 140 kV) with iMAR (protocol 6, $p = 0.01$) and SE with iMAR (protocol 2, $p = 0.001$ to 0.01). All iMAR scan protocols exhibited significantly lower streak artifacts compared with the corresponding scans without iMAR ($p = 0.001$ to 0.01). Detailed results are shown in Table II.

Impact of Applied Protocol on Blooming Artifacts

The smallest virtual growth was found for scan protocols 3 (4.40 mm) and 4 (4.54 mm), the SE protocols with a tin filter.

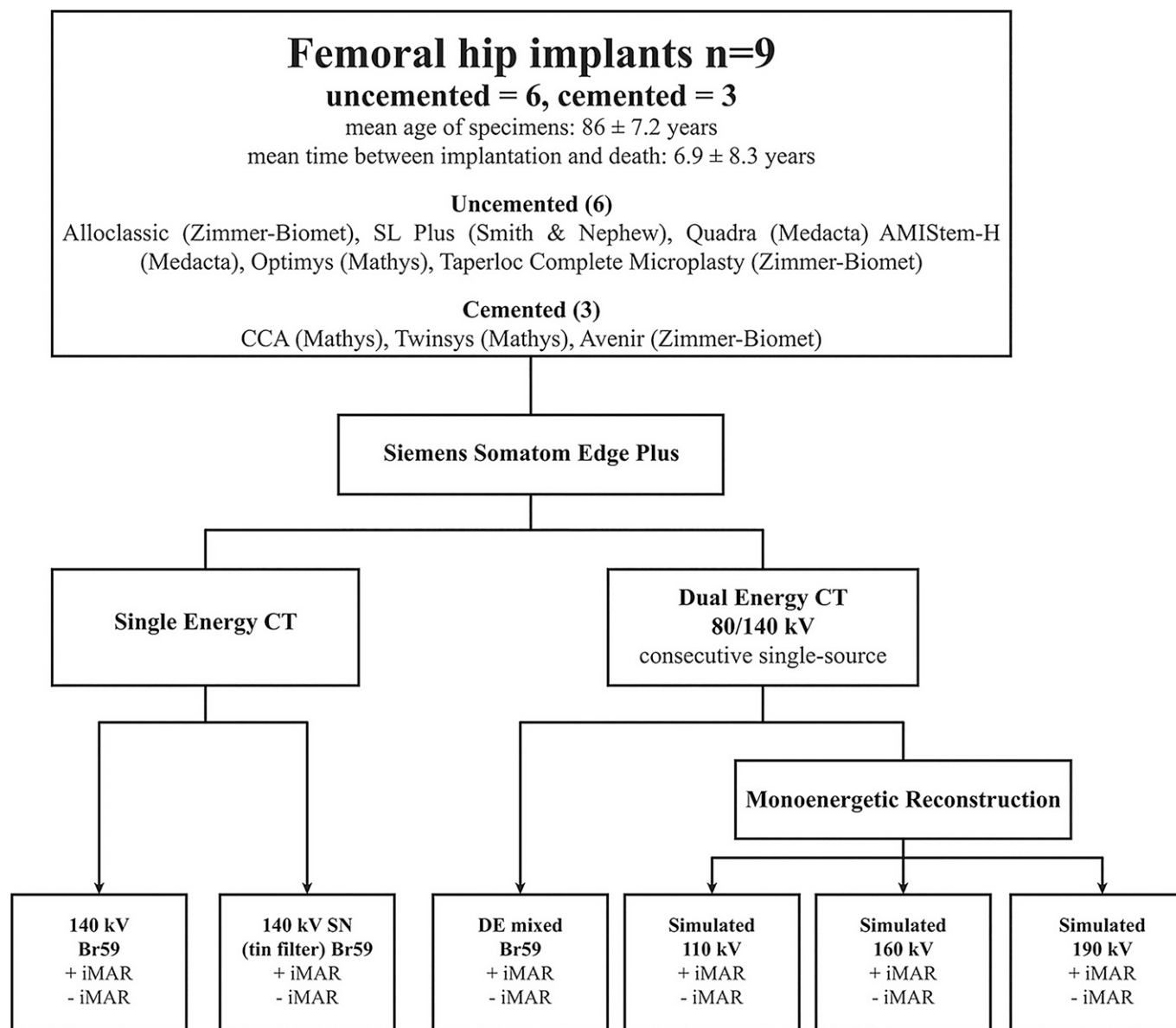


Fig. 3
Overview of the applied CT protocols.

The highest values were observed for scan protocols 5 (7.04 mm) and 6 (6.84 mm), the DE protocols with mixed reconstructions. These differences between protocols 3 and 4 as well as protocols 5 and 6 were significant, with p values of 0.036 to 0.045. Detailed results are shown in Table III.

Impact of Prosthesis and Material

The lowest level of streak artifacts was observed for uncemented standard stems and the highest level, for cemented standard stems. The difference between all uncemented (standard and short) and cemented stems was significant ($p = 0.001$ and 0.015). The difference in blooming artifacts between uncemented and cemented stems was also significant ($p < 0.001$). The smallest virtual growth in cemented stems, 7.97 mm, was

more than 3 times larger than the smallest values in the uncemented group. As shown in Figure 4, the distributions of streak and blooming artifacts among the protocols were similar in all 3 groups.

Qualitative Assessment

The highest-ranked (best) scan protocol in terms of subjective image quality was the SE protocol with a tin filter and iMAR (scan 4), followed by SE with iMAR (scan 2) and monoenergetic reconstruction of 190 keV with iMAR (Fig. 5). The lowest-ranked protocols were those without iMAR, irrespective of whether they were SE or DE. Ranking was similar between cemented and uncemented stems. Detailed rankings are shown in Table I.

TABLE I Overview of Applied Protocols with Radiation Doses and Settings*

Protocol	Protocol Name	Tube Voltages (kV)	iMAR	Slice Thickness/Interval (mm)	Mean Actual mAs/ Mean Ref. mAs	Mean DLP (mGy-cm)	Subjective Image Quality Grade†	Subjective Ranking‡
1	SE	140	Off	0.6/0.6	92.1/150	462.4	4.0	11
2	SE	140	On	0.6/0.6	92.1/150	462.4	1.8	2
3	SE Sn (tin filter)	140	Off	0.6/0.6	413.8/520	446.1	3.4	7
4	SE Sn (tin filter)	140	On	0.6/0.6	413.8/520	446.1	1.3	1
5	DE	80/140	Off	0.6/0.6	280.1/357.9	482.8	4.7	12
6	DE	80/140	On	0.6/0.6	280.1/357.9	482.8	2.6	5
7	Monoenerg. Plus 110	110	Off	0.6/0.6	280.1/357.9	482.8	3.9	10
8	Monoenerg. Plus 160	160	Off	0.6/0.6	280.1/357.9	482.8	3.9	9
9	Monoenerg. Plus 190	190	Off	0.6/0.6	280.1/357.9	482.8	3.9	8
10	Monoenerg. Plus 110	110	On	0.6/0.6	280.1/357.9	482.8	2.5	4
11	Monoenerg. Plus 160	160	On	0.6/0.6	280.1/357.9	482.8	2.5	6
12	Monoenerg. Plus 190	190	On	0.6/0.6	280.1/357.9	482.8	2.5	3

*iMAR = iterative metal artifact reduction algorithm, mAs = milliampere seconds, DLP = dose length product. †On a 5-point Likert scale, with 1 being the best and 5 the worst grade. For all reconstructions, CARE Dose was activated and the BR59 kernel was used. The terms “Monoenergetic Plus” and “iMAR” refers to the Siemens Healthineers protocol names. ‡A ranking of 1 indicates the best image quality and 12, the worst quality.

Discussion

This study investigated the effects of various CT protocols and MAR strategies on CT scans of THAs containing various materials. We compared single-source consecutive DE scans with and without monoenergetic reconstructions and SE protocols with and without a tin filter, all with and without iMAR, using actual bone-implant interfaces in body donors. Analyses employed a phantom water bath setting

with a similar imaging geometry mimicking the surrounding tissue of the thigh in terms of diameter and attenuation. This setup allowed the use of various scan protocols without dose consideration as well as direct quantification of streak and blooming artifacts. Our main findings were that all protocols with iMAR yielded better image quality than the corresponding ones without iMAR, and that the best protocol overall was the SE protocol with a tin filter and iMAR. While

TABLE II Streak Artifacts for Each Protocol and Prosthesis Category*

Scan	Scan Protocol	Uncemented Standard Stem		Uncemented Short Stem		Cemented Standard Stem		Overall	
		HU SD	Rank	HU SD	Rank	HU SD	Rank	HU SD	Rank
1	SE 140 kV	268.6	11	274.8	11	538.9	11	360.8	11
2	SE 140 kV & iMAR	117.9	5	188.5	5	272.2	5	192.9	5
3	SE 140 kV Sn (tin filter)	209.6	10	221.1	9	461.7	10	297.5	10
4	SE 140 kV Sn (tin filter) & iMAR	100.0	3	168.6	4	221.9	4	163.5	4
5	DE 80/140 kV mixed	423.9	12	428.9	12	695.8	12	516.2	12
6	DE 80/140 kV mixed & iMAR	131.0	8	237.2	10	415.9	8	261.3	8
7	Monoenerg. Plus 110 keV	158.0	9	205.9	8	432.0	9	265.3	9
8	Monoenerg. Plus 160 keV	128.0	6	192.2	6	341.5	7	220.6	7
9	Monoenerg. Plus 190 keV	130.1	7	199.6	7	325.3	6	218.3	6
10	Monoenerg. Plus 110 keV & iMAR	95.1	1	165.8	3	207.4	3	156.1	3
11	Monoenerg. Plus 160 keV & iMAR	99.6	2	152.8	2	178.7	1	143.7	1
12	Monoenerg. Plus 190 keV & iMAR	102.7	4	149.9	1	180.5	2	144.4	2

*The standard deviation (SD) of the Hounsfield unit (HU) values was used to quantify streak artifacts; higher values represent higher artifact levels. The corresponding image quality rankings, from 1 (best) to 12 (worst), are based on the HU SDs for the protocols.

TABLE III Blooming Artifacts for Each Group*

Scan	Scan Protocol	Uncemented Straight Stem		Uncemented Short Stem		Cemented Straight Stem		Overall	
		Growth (mm)	Rank	Growth (mm)	Rank	Growth (mm)	Rank	Growth (mm)	Rank
1	SE 140 kV	3.89	8	3.03	6	9.96	10	5.62	9
2	SE 140 kV & iMAR	4.19	10	3.44	10	9.88	9	5.84	10
3	SE 140 kV Sn (tin filter)	2.83	1	2.12	1	8.26	4	4.40	1
4	SE 140 kV Sn (tin filter) & iMAR	3.07	2	2.25	2	8.29	5	4.54	2
5	DE 80/140 kV mixed	5.68	12	4.44	12	11.01	11	7.04	12
6	DE 80/140 kV mixed & iMAR	5.08	11	4.32	11	11.13	12	6.84	11
7	Monoenerg. Plus 110 keV	3.65	5	2.97	5	9.61	8	5.41	8
8	Monoenerg. Plus 160 keV	3.55	4	2.79	3	8.29	6	4.87	4
9	Monoenerg. Plus 190 keV	3.23	3	2.82	4	7.97	1	4.67	3
10	Monoenerg. Plus 110 keV & iMAR	4.05	9	3.43	9	8.22	3	5.23	7
11	Monoenerg. Plus 160 keV & iMAR	3.71	6	3.10	7	8.75	7	5.19	6
12	Monoenerg. Plus 190 keV & iMAR	3.78	7	3.10	8	8.18	2	5.02	5

*The mean virtual growth (in anteroposterior + mediolateral diameters) was used to quantify blooming artifacts; higher values represent higher levels of blooming. The corresponding image quality rankings, from 1 (best) to 12 (worst), are based on the virtual growth in stem size for the protocols.

monoenergetic reconstructions of 160 and 190 keV with iMAR exhibited slightly but not significantly lower levels of streak artifacts, the SE protocol with a tin filter and iMAR exhibited the best results in terms of subjective image quality as well as blooming artifacts.

Imaging is an essential part of the routine follow-up of patients after THA, and usually involves radiographs. However, the information provided by radiographs may be inadequate in cases of periprosthetic loosening or periprosthetic fractures, and CT with artifact reduction may be required for further assessment. However, most previous studies of optimal CT scan parameters have used artificial setups with simulated bone and soft tissue^{9,20} or simplified animal models¹⁴. Selles et al.⁹ used a THA phantom setup and found that virtual monoenergetic imaging of 130 keV with MAR algorithms provided stronger artifact reduction compared with conventional 140-kV images. Bongers et al.⁷ and Neuhaus et al.¹² did analyze CT scans from patients, but they were unable to compare multiple protocols due to dose restrictions^{7,21}. They reported that the combination of virtual monoenergetic imaging with MAR algorithms yielded the greatest decrease in artifacts.

We aimed to add knowledge to the existing literature by assessing the optimal CT protocol for patients with a THA by using a realistic ex vivo setting, which has not been previously described in the literature to our knowledge. Each hip stem had been implanted during the person's lifetime, and thus represented the actual bone-implant interface for the first time. Furthermore, the included prostheses displayed different stages of osseointegration, and the mean donor age was similar to the peak of periprosthetic fractures¹⁶. We found that the best overall protocol in terms of subjective image quality was the SE protocol with a tin

filter and iMAR. As previously reported, the tin filter hardens the x-ray beam, narrowing its energy spectrum to higher levels, and thus would logically be expected to reduce beam-hardening effects that occur around a metal prosthesis⁸. It is important to note that the present study focused on the visualization of the bone-implant interface. The protocol with the best subjective image quality (140 kV with a tin filter and iMAR), however, has the drawback that it would result in decreased iodine contrast compared with standard CT tube voltages (120 kV). Therefore, if iodine enhancement is required, e.g., for visualization of an additional suspected abscess or mass, use of DE scans with monoenergetic reconstructions and MAR is advisable.

Monoenergetic reconstructions of single-source consecutive DE at levels of 110, 160, and 190 keV also resulted in slightly reduced streak artifacts compared with conventional mixed DE images of 80 and 140 kV but did not perform as well in the subjective image evaluation. While monoenergetic reconstructions were superior when iMAR was not used, the difference compared with SE scans with a tin filter became insignificant when iMAR was in use. MAR algorithms such as iMAR were developed to reduce artifacts around metalwork and they have been highly effective in this regard, as demonstrated in the realistic setting in this study. All protocols in which iMAR was activated showed significantly reduced streak artifacts compared with the corresponding non-iMAR protocol, which is consistent with previous clinical and phantom studies^{9,20}.

In contrast, iMAR did not significantly reduce blooming artifacts. The best protocol regarding blooming was again SE scanning with a tin filter, followed by the monoenergetic reconstructions of 190 and 160 keV. The pattern of blooming artifact sizes among the scan protocols was similar for all 3 stem types, but

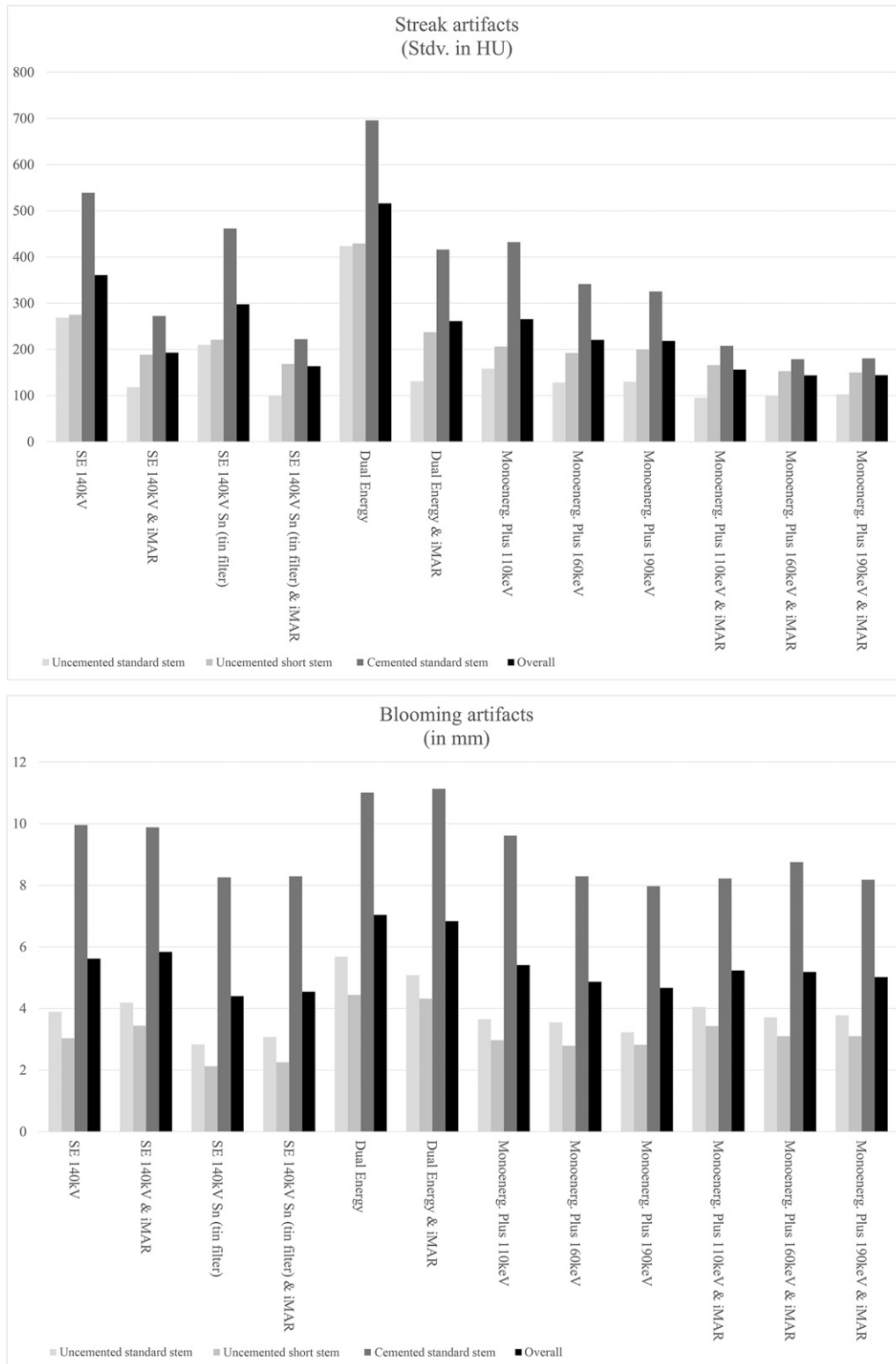


Fig. 4

Distributions of streak (*top*) and blooming artifacts (*bottom*) for each protocol and group. Streak artifact values represent the standard deviation of the Hounsfield units, and blooming artifact values represent the virtual growth in the diameter of the stem. The best image quality results were seen for the single-energy (SE) protocol with a tin filter and iterative metal artifact reduction (iMAR) and for the Monoenergetic Plus reconstructions of 110, 160, and 190 keV with iMAR.

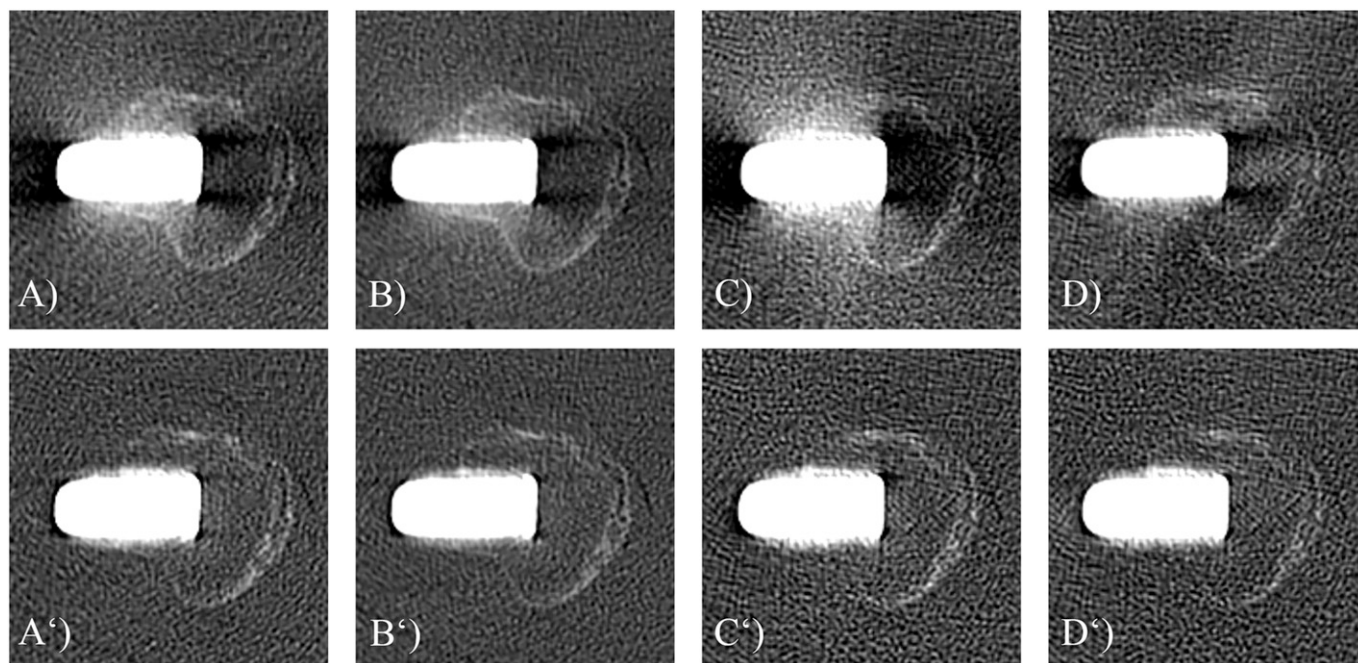


Fig. 5
Visual comparison of the best protocols according to streak and blooming artifacts as well as subjective evaluation. **Fig. 5-A** Single energy. **Fig. 5-B** Single energy with a tin filter. **Fig. 5-C** Dual energy, 80/140 kV mixed. **Fig. 5-D** Monoenergetic Plus at 190 keV. **Figs. 5-A' through 5-D'** The corresponding images with iterative metal artifact reduction (iMAR).

cemented stems revealed significantly larger virtual growth overall. This can be explained by the difference in metal alloys. Uncemented stems primarily consist of titanium, whereas cemented stems are primarily stainless-steel alloys. These findings are consistent with previous phantom studies^{8,22} and demonstrate a potential disadvantage of cemented stems in the evaluation of prosthetic loosening or periprosthetic fracture with CT scans.

MAR algorithms are also commonly used in magnetic resonance imaging (MRI)²³. However, while MRI is useful for detecting cysts and solid masses caused by wear particles, its ability to evaluate the bone-implant interface has limitations. In cases of prosthetic loosening or a possible occult periprosthetic fracture, additional CT with a MAR algorithm is the best imaging option to visualize the bone-implant interface. Our study suggests that this algorithm can be successfully used for both DE and SE scans, and it does not require additional radiation exposure. The improved image quality when visualizing the bone-implant interface might help clinicians to more rapidly arrive at the correct diagnosis and design an accurate treatment.

The primary limitation to generalizing the results of the present study involves the specimens that were included, which were dependent on the availability of specimens at our institution. Although we included 9 different hip stems from different manufacturers, there are many more systems on the market. Nevertheless, we included as many different stems as possible to cover a broad spectrum of the available products and alloys on the market. Another possible limitation of our setup is the use of a single CT scanner and a single DE technique and corresponding iterative MAR (iMAR). The presented

results cannot be fully extrapolated to other scanners, as each company producing CT scanners provides its own metal artifact algorithm. Nevertheless, the single-source DE scanner used in this study is widely used in orthopaedic hospitals and will remain the workhorse for many years to come, and all commercially available algorithms are based on the same basic principle⁶. Another potential limitation is the chosen method of quantitative streak artifact measurement using several ROIs placed around the prosthesis. Although this method has not been established as the standard for streak-artifact measurement, it has been used in previous studies and described in more detail there⁸.

The key strength of this study is the unique characteristics of our specimens studied in a realistic setup. All prostheses were implanted during the individual's lifetime, and consequently provide a realistic representation of the osseointegration of femoral stems. Previous studies that used artificial settings could not simulate osseointegration and the changes that occur in the bone over time. To our knowledge, this is the first comprehensive study comparing different CT protocols for assessing femoral stems with secondary fixation (i.e., osseointegration).

In conclusion, the results of this study suggest that MAR algorithms (e.g., iMAR) should be used in clinical practice for imaging of the bone-implant interface of prostheses with either an uncemented or cemented femoral stem. Among the protocols in which iMAR was active, the SE protocol with 140 kV and a tin filter produced the best subjective image quality. Furthermore, this protocol and DE monoenergetic reconstructions of 160 and 190 keV with iMAR achieved the lowest levels of streak and blooming artifacts. ■

NOTE: The authors thank the assistant prosectors at the Division of Anatomy, Center for Anatomy and Cell Biology, of the Medical University of Vienna for the collection and preparation of the body donor specimens, as well as Andreas Mikats. The authors also thank the body donors and their families; without their selfless contribution, this work would not have been possible.

Gilbert M. Schwarz, MD^{1,2,3}
Stephanie Huber, MD^{2,3}
Christian Wassipaul, MD⁴
Maximilian Kasperek, MD, PhD⁵
Lena Hirtler, MD, PhD²
Jochen G. Hofstaetter, MD^{2,6}
Till Bader, MD⁷
Helmut Ringl, MD^{4,8}

¹Department of Orthopedics and Trauma-Surgery, Medical University of Vienna, Vienna, Austria

²Center for Anatomy and Cell Biology, Medical University of Vienna, Vienna, Austria

³Michael Ogon Laboratory for Orthopedic Research, Orthopedic Hospital Vienna, Vienna, Austria

⁴Department of Biomedical Imaging and Image-Guided Therapy, Medical University of Vienna, Vienna, Austria

⁵Lutheran Hospital Vienna (Evangelisches Krankenhaus), Vienna, Austria

⁶2nd Department, Orthopedic Hospital Vienna, Vienna, Austria

⁷Department of Radiology, Orthopedic Hospital Vienna, Vienna, Austria

⁸Department of Radiology, Clinics Donaustadt, Vienna, Austria

Email for corresponding author: lena.hirtler@meduniwien.ac.at

References

- Zhang Y, Jordan JM. Epidemiology of osteoarthritis. *Clin Geriatr Med*. 2010 Aug; 26(3):355-69.
- WHO Scientific Group on the Burden of Musculoskeletal Conditions at the Start of the New Millennium. The burden of musculoskeletal conditions at the start of the new millennium. *World Health Organ Tech Rep Ser*. 2003;919:i-x, 1-218, back cover.
- Singh JA. Epidemiology of knee and hip arthroplasty: a systematic review. *Open Orthop J*. 2011 Mar 16;5:80-5.
- Mushtaq N, To K, Gooding C, Khan W. Radiological Imaging Evaluation of the Failing Total Hip Replacement. *Front Surg*. 2019 Jun 18;6:35.
- Roth TD, Maertz NA, Parr JA, Buckwalter KA, Choplin RH. CT of the hip prosthesis: appearance of components, fixation, and complications. *Radiographics*. 2012 Jul-Aug;32(4):1089-107.
- Katsura M, Sato J, Akahane M, Kunimatsu A, Abe O. Current and Novel Techniques for Metal Artifact Reduction at CT: Practical Guide for Radiologists. *Radiographics*. 2018 Mar-Apr;38(2):450-61.
- Bongers MN, Schabel C, Thomas C, Raupach R, Notohamiprodjo M, Nikolaou K, Bamberg F. Comparison and Combination of Dual-Energy- and Iterative-Based Metal Artefact Reduction on Hip Prosthesis and Dental Implants. *PLoS One*. 2015 Nov 24; 10(11):e0143584.
- Kasperek MF, Töpker M, Lazar M, Weber M, Kasperek M, Mang T, Apfalter P, Kubista B, Windhager R, Ringl H. Dual-energy CT and ceramic or titanium prostheses material reduce CT artifacts and provide superior image quality of total knee arthroplasty. *Knee Surg Sports Traumatol Arthrosc*. 2019 May;27(5):1552-61.
- Selles M, Stuijvenberg VH, Wellenberg RHH, van de Riet L, Nijholt IM, van Osch JAC, van Hamersvelt RW, Leiner T, Boomsma MF. Quantitative analysis of metal artifact reduction in total hip arthroplasty using virtual monochromatic imaging and orthopedic metal artifact reduction, a phantom study. *Insights Imaging*. 2021 Nov 24;12(1):171.
- Wellenberg RH, Boomsma MF, van Osch JA, Vlassenbroek A, Milles J, Edens MA, Streekstra GJ, Slump CH, Maas M. Low-dose CT imaging of a total hip arthroplasty phantom using model-based iterative reconstruction and orthopedic metal artifact reduction. *Skeletal Radiol*. 2017 May;46(5):623-32.
- Wellenberg RHH, Hakvoort ET, Slump CH, Boomsma MF, Maas M, Streekstra GJ. Metal artifact reduction techniques in musculoskeletal CT-imaging. *Eur J Radiol*. 2018 Oct;107:60-9.
- Neuhaus V, Grosse Hokamp N, Zopfs D, Laukamp K, Lennartz S, Abdullayev N, Maintz D, Borggrefe J. Reducing artifacts from total hip replacements in dual layer detector CT: Combination of virtual monoenergetic images and orthopedic metal artifact reduction. *Eur J Radiol*. 2019 Feb;111:14-20.
- Horat L, Hamie MQ, Huber FA, Guggenberger R. Optimization of Monoenergetic Extrapolations in Dual-Energy CT for Metal Artifact Reduction in Different Body Regions and Orthopedic Implants. *Acad Radiol*. 2019 May;26(5):e67-74.
- Huber FA, Sprengel K, Müller L, Graf LC, Osterhoff G, Guggenberger R. Comparison of different CT metal artifact reduction strategies for standard titanium and carbon-fiber reinforced polymer implants in sheep cadavers. *BMC Med Imaging*. 2021 Feb 15;21(1):29.
- Evans JT, Evans JP, Walker RW, Blom AW, Whitehouse MR, Sayers A. How long does a hip replacement last? A systematic review and meta-analysis of case series and national registry reports with more than 15 years of follow-up. *Lancet*. 2019 Feb 16;393(10172):647-54.
- Scalici G, Boncinelli D, Zanna L, Buzzi R, Antonucci L, Di Maida F, De Biase P. Periprosthetic femoral fractures in Total Hip Arthroplasty (THA): a comparison between osteosynthesis and revision in a retrospective cohort study. *BMC Musculoskelet Disord*. 2022 Mar 3;23(1):200.
- Gruen TA, McNeice GM, Amstutz HC. "Modes of failure" of cemented stem-type femoral components: a radiographic analysis of loosening. *Clin Orthop Relat Res*. 1979 Jun;(141):17-27.
- Su AW, Hillen TJ, Eutsler EP, Bedi A, Ross JR, Larson CM, Clohisey JC, Nepple JJ. Low-dose CT reduces radiation exposure by ninety percent compared to traditional CT among patients undergoing hip preservation surgery. *Arthroscopy*. 2019 May; 35(5):1385-92.
- Cicchetti DV, Sparrow SA. Developing criteria for establishing interrater reliability of specific items: applications to assessment of adaptive behavior. *Am J Ment Defic*. 1981 Sep;86(2):127-37.
- Wellenberg RHH, Boomsma MF, van Osch JAC, Vlassenbroek A, Milles J, Edens MA, Streekstra GJ, Slump CH, Maas M. Computed Tomography Imaging of a Hip Prosthesis Using Iterative Model-Based Reconstruction and Orthopaedic Metal Artefact Reduction: A Quantitative Analysis. *J Comput Assist Tomogr*. 2016 Nov/Dec;40(6):971-8.
- Zhang K, Han Q, Xu X, Jiang H, Ma L, Zhang Y, Yang K, Chen B, Wang J. Metal artifact reduction of orthopedics metal artifact reduction algorithm in total hip and knee arthroplasty. *Medicine (Baltimore)*. 2020 Mar;99(11):e19268.
- Vellarackal AJ, Kaim AH. Metal artefact reduction of different alloys with dual energy computed tomography (DECT). *Sci Rep*. 2021 Jan 26;11(1):2211.
- Kwon YM. Cross-sectional imaging in evaluation of soft tissue reactions secondary to metal debris. *J Arthroplasty*. 2014 Apr;29(4):653-6.